ACS Catalysis

Research Article

Cite This: ACS Catal. 2019, 9, 746−754

pubs.acs.org/acscatalysis

Mn-Catalyzed Electrochemical Chloroalkylation of Alkenes

Niankai Fu,[†] Yifan Shen,[†] Anthony R. Allen,[†,‡] Lu Song,[†] Atsushi Ozaki,[†,§] and Song Lin*[,†]

[†]Department of Chemistry and Chemical Biology, Cornell University, Ithaca, New York 14853, United States

[‡]Department of Chemistry and Biochemistry, Oberlin College, Oberlin, Ohio 44074, United States

[§]Department of Applied Biological Science, Tokyo University of Agriculture and Technology, Fuchu, Tokyo 183-8509, Japan

Supporting Information

ABSTRACT: The heterodifunctionalization of alkenes is an efficient method for synthesizing highly functionalized organic molecules. In this report, we describe the use of anodically coupled electrolysis for the catalytic chloroalkylation of alkenes—a reaction that constructs vicinal C−C and C−Cl bonds in a single synthetic operation—from malononitriles or cyanoacetates and NaCl. Knowledge of the persistent radical effect guided the reaction design and development. A series of controlled experiments, including divided-cell electrolysis that compartmentalized the anodic and cathodic events, allowed us to identify the key radical intermediates and the pathway to their electrocatalytic formation. Cyclic voltammetry data further support the proposed mechanism entailing the parallel, Mn-mediated generation of two radical intermediates in an anodically coupled electrolysis followed by their selective addition to the alkene.

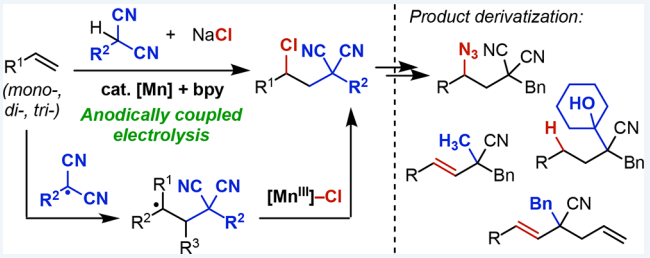

KEYWORDS: *electrocatalysis, electrosynthesis, chloroalkylation, alkene difunctionalization, anodically coupled electrolysis*

INTRODUCTION

Owing to the prevalence of C=C bonds in feedstock chemicals and naturally occurring materials, the heterodifunctionalization of alkenes provides an efficient strategy for rapidly increasing the complexity of molecules in organic synthesis.[1] For example, the haloalkylation of alkenes[2] leads to the formation of vicinal C−C and C−X bonds in the same transformation, extending the carbon chain and providing an alkyl halide functional handle for further synthetic elaborations. In this context, the Kharasch addition reaction represents an efficient approach to the haloalkylation of alkenes using homolytically labile alkyl halides (e.g., iodo/bromoalkanes and CCl_4).[3,4] However, the extension of this radical strategy to chloroalkylation with less reactive alkyl chlorides is challenged by the relatively high dissociation energy of C−Cl bonds in these electrophiles. To date, such an endeavor has been limited to intramolecular cyclizations using polychlorinated substrates (Scheme 1A).[5] New approaches that could enable this transformation in an intermolecular fashion using common starting materials would provide access to a broader array of densely functionalized molecules for applications in organic synthesis and medicinal chemistry.

Mn(III)-promoted oxidative radical cyclization of 1,3-dicarbonyl compounds to alkenes[6] is a powerful approach to constructing C−C bonds en route to complex target products (Scheme 1B).[7,8] In a related context, we recently developed Mn-catalyzed electrochemical methods[9] for the difunctionalization of alkenes.[10] This strategy combines the electrochemical generation of radical intermediates followed by catalyst-controlled addition of these nascent open-shell species

Scheme 1. Chloroalkylation of Alkenes: the Kharasch Addition vs the Electrocatalytic Approach

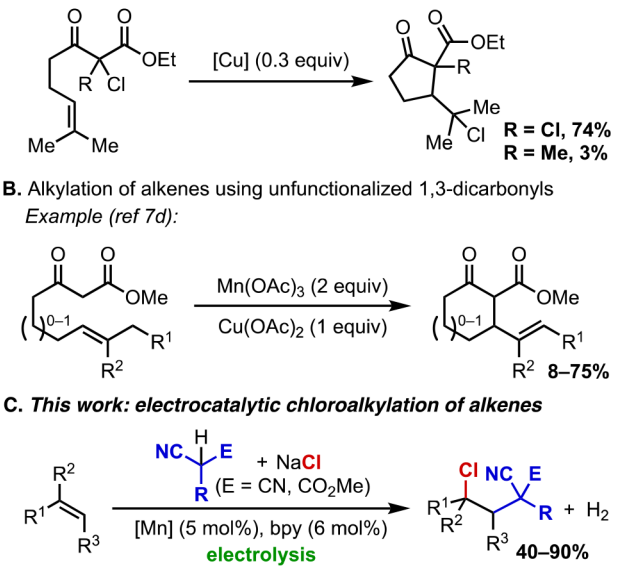

Received: August 13, 2018
Revised: November 4, 2018
Published: December 5, 2018

DOI: 10.1021/acscatal.8b03209
ACS Catal. 2019, 9, 746−754

across the alkene π-bond. The merger of electrochemistry and redox metal catalysis allows such reactions to occur under mild conditions with a broad substrate scope and high regio- and chemoselectivity. In particular, we demonstrated anodically coupled electrolysis[10a,c]—a process that combines two distinct oxidation events in parallel—for the regioselective chlorotrifluoromethylation of alkenes. Herein, we report the application of this new catalytic strategy in the intermolecular chloroalkylation of simple alkenes using unfunctionalized malononitriles or cyanoacetates and NaCl (Scheme 1C).

RESULTS AND DISCUSSION

A. Reaction Design and Development. We reasoned that anodically coupled electrolysis could be applied to the chloroalkylation of alkenes. Related previous work showed that α-C−H oxidation of 1,3-dicarbonyl compounds can be effected by a metal oxidant such as $Mn(OAc)_3$ to generate the corresponding carbon-centered radicals (**I**) (Scheme 2A, eq 1).[7,8] This reactivity was used elegantly for C−C bond construction with alkenes followed by radical elimination or intramolecular cyclization. Furthermore, we have demonstrated the formation of $[Mn^{III}]$−Cl (**II**) as the latent Cl radical from Cl^- and Mn^{II} in the Mn-catalyzed electrochemical chlorination reactions (Scheme 2A, eq 2).[10c,d] We hypothesized that, upon the formation of **I** and **II**, the intrinsic reactivity profiles of these radical intermediates would lead to their chemo- and regioselective addition to the alkene substrate (Scheme 2B). Specifically, the alkene will preferentially react with transient radical **I** to construct a new C−C bond, forming transient radical **III**. Subsequently, the capture of **III** by persistent radical **II** will occur selectively[11] to complete the desired chloroalkylation.

Guided by this general design principle, we aimed to develop a chloroalkylation reaction using 4-*tert*-butylstyrene (**1**) as the alkene substrate, benzyl malononitrile (**2**) as the C donor, and a chloride salt as the Cl donor. Multiple iterations of optimization resulted in highly efficient and selective reaction conditions comprising $Mn(OTf)_2$ as the precatalyst, 2,2′-bipyridine (bpy) as the ligand, NaCl as the Cl donor, and $LiClO_4$ as the electrolyte in a mixture of HOAc and MeCN at 50 °C. With carbon felt, a porous and commercially available material, as the anode and a Pt plate, an efficient material for proton reduction, as the cathode, the application of a 6.0 mA current (2 F total charge) furnished the desired three-component adduct **3** in 94% yield (corresponding to 94% current efficiency) with only traces of 1,2-dichloride **4** as a side product (Table 1, entry 1). In the absence of Mn, no chloroalkylation reactivity was observed, and 10% of **4** was formed (entry 2). In the absence of bpy, the desired heterodifunctionalization proceeded at a slower rate (entry 3) and was accompanied by various side reactions including dichlorination. The role of bpy cannot be explained simply as that of a base, as the addition of pyridine instead of bpy did not provide the high reactivity observed under the optimal conditions (entry 4 vs entry 1).

The electrocatalytic chloroalkylation was also successful under controlled potential conditions. With a full cell voltage of 2.3 V (entry 5) or an anodic potential of 0.62 V (vs ferrocenium/ferrocene, $Fc^{+/0}$; entry 6), product **3** was formed in high yield and high selectivity. We also surveyed various chloride sources and found that more soluble salts such as $MgCl_2$ resulted in rapid dichlorination activity that completely outcompeted the chloroalkylation (entry 7). We reason that the low solubility of NaCl ensured a low concentration of $[Mn^{III}]$−Cl, the putative radical chlorinating agent, which resulted in preferential inhibition of the side dichlorination pathway and, thus, higher chemoselectivity.[12] The identity of the electrolyte proved unimportant to the reaction outcome:

Scheme 2. Design Principle for the Electrochemical Alkylchlorination of Alkenes[a]

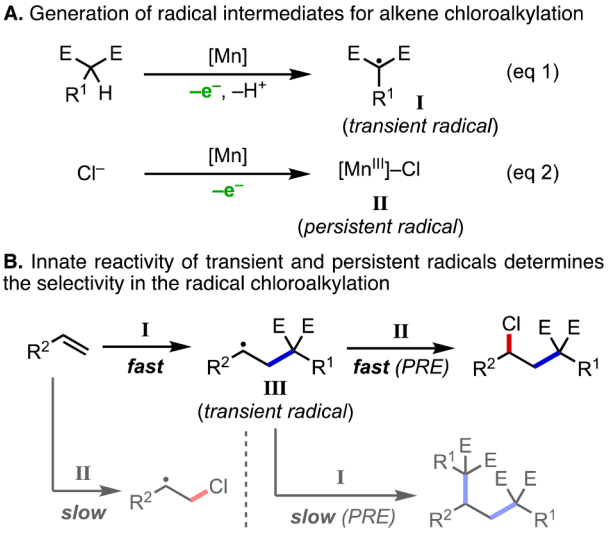

[a]E = electron-withdrawing group. PRE = persistent radical effect.

Table 1. Reaction Optimization[a]

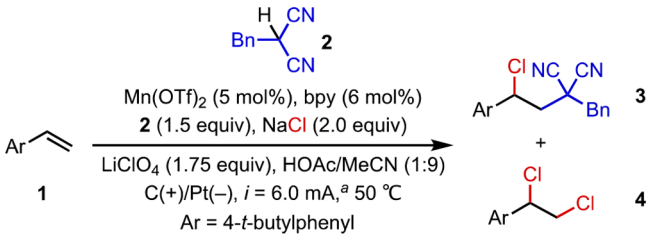

entry	variation from the standard conditions	yield[b] (%) 3	4
1	**none**	**94**	**<5**
2	without $Mn(OTf)_2$	<5	10
3	without bpy	46	12
4	12 mol % pyridine instead of bpy	47	5
5	control cell voltage at 2.3 V[c]	84	14
6	Control anode potential at 0.62 V[d]	88	<5
7	$MgCl_2$ instead of NaCl	<5	>99
8	$Et_4N^+OTs^-$ or $TBAPF_6$ instead of $LiClO_4$	87−90	<5
9	Ni foam instead of Pt as cathode	70	<5
10	40 °C instead of 50 °C	68	<5
11	i = 4.0 mA	91	<5
12	i = 8.0 mA	80	<5

[a]Current controlled at 6.0 mA throughout the electrolysis. Reaction was stopped after 1 h and 47 min after the passage of 2 F of charge. [b]Yields were determined with ^1H NMR using 1,3,5-trimethoxybenzene as the internal stardard. [c]The cell voltage was kept constant for 2 h. The current varied between 12 and 6 mA during the reaction course. [d]The anode potential was kept constant at 0.62 V vs $Fc^{+/0}$ for 2 h.

DOI: 10.1021/acscatal.8b03209
ACS Catal. 2019, 9, 746−754

Scheme 3. Substrate Scope*

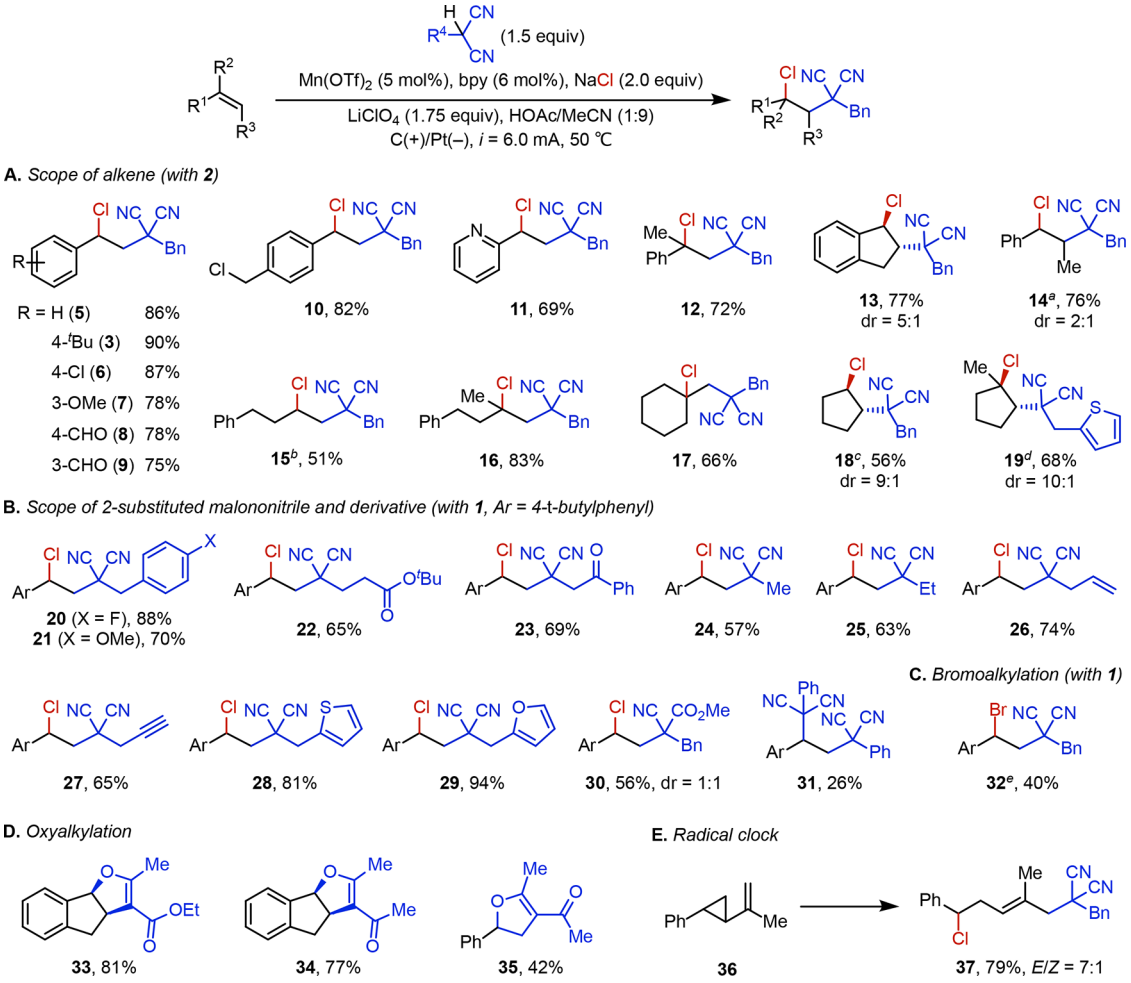

*All substrates were electrolyzed at 6.0 mA after 2 F charge was passed; Faradaic yield = product yield. [a]From (*E*)-*β*-methylstyrene. [b]2.5 F charge was passed, Faradaic yield = 41%. [c]Electrolysis at a constant cell voltage of 2.3 V for 2 h. [d]Using the malononitrile as the limiting substrate (1 equiv) in combination with 1.5 equiv of **1**. [e]Using NaBr instead of NaCl at room temperature; 3 F charge was passed, Faradaic yield = 27%.

$Et_4N^+OTs^-$ and $Bu_4N^+PF_6^-$ provided practically the same yield and selectivity (entry 8). We also found that the use of inexpensive Ni foam as the cathode material instead of Pt afforded **3** in synthetically useful yield (entry 9).

B. Substrate Scope. We then investigated the substrate scope of the reaction (Scheme 3). A variety of styrene-type substrates were converted to chloroalkylated products (**3**, **5**–**14**) in high yields under the optimal conditions. In particular, aldehyde (**8**, **9**) and benzyl chloride (**10**) groups were well-tolerated, and we found no evidence of formyl group oxidation or nucleophilic displacement of the alkyl halide by **2**. Substituted styrenes such as *α*- and *β*-methylstyrene (**12**, **14**) and indene (**13**) were converted to the desired products with good efficiency.

Aliphatic alkenes also proved suitable substrates. Terminal alkenes participated smoothly in the desired transformation (**15**–**17**). Owing to the large steric profile of **2**, acyclic alkenes with other substitution patterns, including 1,2-disubstituted, trisubstituted, and tetrasubstituted alkenes, showed only low levels of reactivity. Nevertheless, cyclic alkenes such as cyclopentene and 1-methylcyclopentene underwent strain-relieving difunctionalization to furnish the corresponding products (**18** and **19**) in synthetically useful yield and high diastereoselectivity favoring the trans isomers.

We then explored the reaction scope of the alkylating agent. A variety of substituted malononitriles were reacted under the optimal electrolysis conditions to furnish the three-component adducts in good to excellent yields. In particular, enolizable esters and ketones, groups that could potentially compete with the malononitrile in the chloroalkylation, were preserved during the reaction (**22** and **23**). In addition, allyl and propargyl malononitrile were compatible with the reaction (**26** and **27**), in which the styrenyl C═C bond was preferentially functionalized. Finally, heterocycles including thiophene (**28**) and furan (**29**) were well-tolerated.

We further extended the reaction scope to methyl 2-benzylcyanoacetate, which furnished product **30** in good yield. Cyanoacetates are, however, unreactive toward aliphatic alkenes. 2-Phenylmalononitrile reacted with *tert*-butylstyrene to give bisalkylation product **31** in 26% yield. This product most likely arose from the desired chloroalkylation followed by nucleophilic substitution of the benzyl chloride by the C nucleophile. Indeed, a control experiment with an excess of *tert*-butylstyrene relative to 2-phenylmalononitrile provided predominantly the corresponding chloroalkylation product as observed by ^{1}H NMR.

Furthermore, by replacing NaCl with NaBr and conducting the electrolysis at a lower temperature, bromoalkylation

DOI: 10.1021/acscatal.8b03209
ACS Catal. 2019, 9, 746–754

product **32** could be obtained in a synthetically useful yield in addition to a small amount of the corresponding dibromoalkane (Scheme 3C).

Acetylacetone and acetylacetates reacted smoothly with indene under the optimal conditions but delivered 1,2-dihydrofuran-type products (**33**–**35**) instead of the chloroalkylation products (Scheme 3D). These polycyclic products were also formed in the absence of NaCl. Mechanistically, we hypothesized that the carbon-centered radical resulting from radical addition of the 1,3-dicarbonyl intermediate to the alkene was further oxidized to the benzylic carbocation prior to being captured by the adjacent enol. This pathway is likely more favorable with acetylacetone and acetylacetates than with malononitriles because the radical-to-cation oxidation is facilitated by the subsequent nucleophilic cyclization.[13] Finally, extension of the current reaction system to malonates has proven challenging at this stage; alkene dichlorination adducts were often the predominant products in these systems. Cyclic voltammetry data revealed that, similar to malononitriles (see section D), malonates can also be oxidized electrochemically in the presence of Mn (see the SI). As such, it is unlikely that the lack of reactivity with malonates arises from the difficulty in generating the corresponding carbon-centered radicals. In previous studies, it has been proposed that Mn^{III} can coordinate with malonates to form metal-bound radicals in the form of stable Mn-enolates.[6b] Thus, we hypothesize that these enolates are less reactive than the corresponding free-carbon radicals toward alkene addition.

C. Product Derivatization. The chloroalkylation reaction installs two functional handles in a single step for the further construction of structurally complex molecules. We demonstrated the synthetic value of the heterodifunctionalization products in a set of derivatization reactions (Scheme 4). For example, the newly installed C–Cl bond can be substituted by N_3^- (**38**), eliminated to form a C=C bond (**39** and **41**), or reduced to a C–H bond (**43**).

Scheme 4. Derivatization of the Chloroalkylation Products

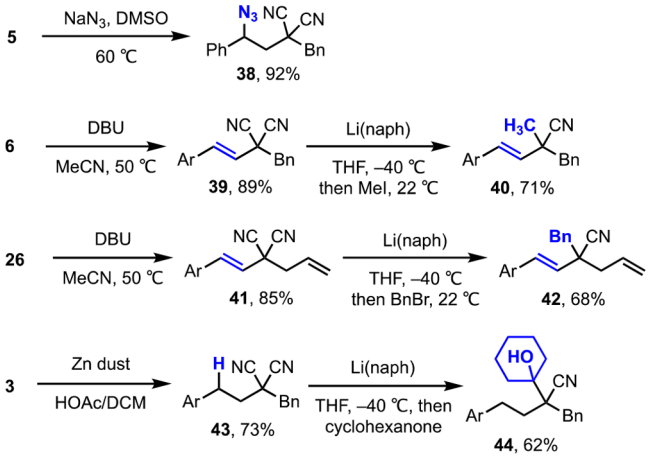

We also exploited the unique reactivity of *gem*-dicyano groups to undergo decyanoalkylation in the presence of Li naphthalide.[14] For example, using MeI or BnBr as the electrophile, products with an all-carbon quaternary stereogenic center (**40** and **42**) could be obtained. This reactivity was also extended to an aldol-type addition reaction with cyclohexanone to form a sterically congested 3° alcohol (**44**).

D. Mechanistic Studies: Control Experiments. The involvement of carbon-centered radical intermediates in the difunctionalization reaction was further supported by a radical clock experiment with cyclopropyl-substituted alkene **36** (Scheme 3E). Upon formation of the first C–C bond, the resultant radical triggered ring rupture of the adjacent cyclopropyl group, which ultimately led to the formation of product **37** in 79% yield.

We propose that the formation of carbon-centered radical **IV** arises from single-electron oxidation of the conjugate anion of **2** in an Mn^{III}-mediated process (see Scheme 2, eq 1). However, two alternative mechanisms are in theory possible, both involving the electrochemical formation of chlorinated malononitrile **45** (Scheme 5). Indeed, our optimal reaction conditions yielded **45** in 53% yield in the absence of alkene **1** (eq 3). This intermediate may undergo Mn-catalyzed Kharasch-type radical addition independent of any electrochemical processes (alternative path 1). Alternatively, upon formation, **45** may diffuse to the cathode and be reduced to

Scheme 5. Alternative Mechanistic Pathways and Control Experiments[a]

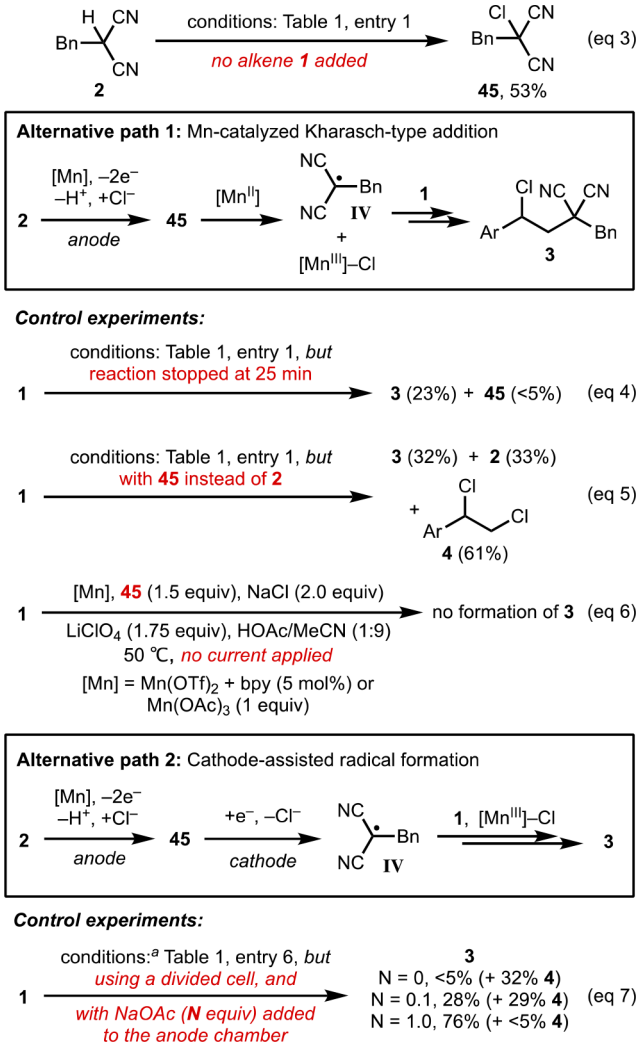

[a]The composition of the anodic compartment was identical to that of the undivided-cell experiment in Table 1, entry 6; the cathodic compartment contained $LiClO_4$, HOAc, and MeCN and was also heated to 50 °C.

DOI: 10.1021/acscatal.8b03209
ACS Catal. 2019, 9, 746–754

radical **IV** prior to its addition to the alkene (alternative path 2).

Control experiments definitively excluded the possibility of a Kharasch-type mechanism (alternative path 1). First, when the electrocatalytic reaction was stopped prematurely, only traces of **45** were observed (eq 4). Furthermore, replacing **2** with **45** as the malononitrile source under otherwise identical conditions led to a different product composition of predominantly dichloride **4** along with 32% **3** and 33% **2** (eq 5). Additional experiments showed that **45** did not participate in the alkene functionalization without the current input in the presence of either Mn^{II} or Mn^{III} (eq 6).

CV and electrolysis experiments showed that, under the electrolysis conditions, **45** can undergo cathodic reduction and mesolytic cleavage of the C−Cl bond to form carbon-centered radical **IV** (see the SI). However, alternative path **2** was ruled out by conducting the electrolysis using a setup that separated the anode from the cathode with an ion-conducting glass frit. This divided-cell system prevented the diffusion of anodically generated **45** to the cathodic compartment. Although initial experiments under the standard conditions yielded only traces of product, the addition of NaOAc in the anodic compartment restored the chloroalkylation reactivity (eq 7). Taken together, these control experiments provide compelling evidence that the alternative pathways mediated by **45**, if operating at all under the reaction conditions, contribute minimally to the observed chloroalkylation reactivity.

Upon addition of **IV**, an electrophile radical, to the alkene, the resultant carbon-centered radical **V** will accept a Cl atom from the putative $[Mn^{III}]$−Cl catalytic intermediate (vide infra), completing the chloroalkylation event. Alternatively, **V** could undergo single-electron oxidation, either directly on the anode or mediated by Mn^{III}, to form the corresponding carbocation. This process is then followed by nucleophilic chlorination with Cl^-. This pathway, however, is unlikely to contribute significantly to the observed reactivity. First, substrates with which the carbocation formation is unfavorable, such as **8**, **11**, and **15**, underwent the chloroalkylation smoothly. Second, in the majority of cases studied, we did not observe competing acetoxylation or Ritter-type amidation of the hypothetical carbocation intermediates. These side reactions would be expected owing to the significantly higher concentration of OAc^- and MeCN in the reaction medium and the comparable nucleophilicity[15] of the former vs Cl^- (16.9 vs 17.2, in MeCN). As an additional piece of evidence against the carbocation pathway, we conducted competition experiments using an equal amount of NaCl and NaCN (nucleophilicity 16.3). Under standard electrolysis conditions, the chloroalkylation product was observed exclusively (Scheme 6); the cyanoalkylation product, which would be expected if the reaction adopts the carbocation mechanism, was not formed. Taken together, we conclude that the radical Cl-atom transfer by Mn is the more likely pathway for the C−Cl bond formation.

Scheme 6. Competition Experiment[a]

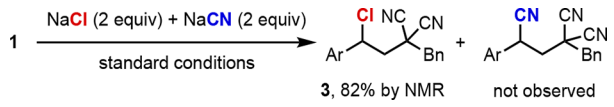

[a]See Table 1, entry 1, for conditions.

E. Cyclic Voltammetry Studies. We carried out CV studies to gain further insights into the reaction mechanism. In particular, we attempted to understand the role Mn, bpy, and NaOAc play in the reaction. In MeCN, neither $Mn(OTf)_2$ nor **2** alone displayed any oxidation event in the 0−1 V (vs $Fc^{+/0}$) potential window.[16] The addition of bpy (1.2 equiv with respective to Mn), however, resulted in the appearance of a new, irreversible anodic feature at ca. 700 mV (Figure 1, black

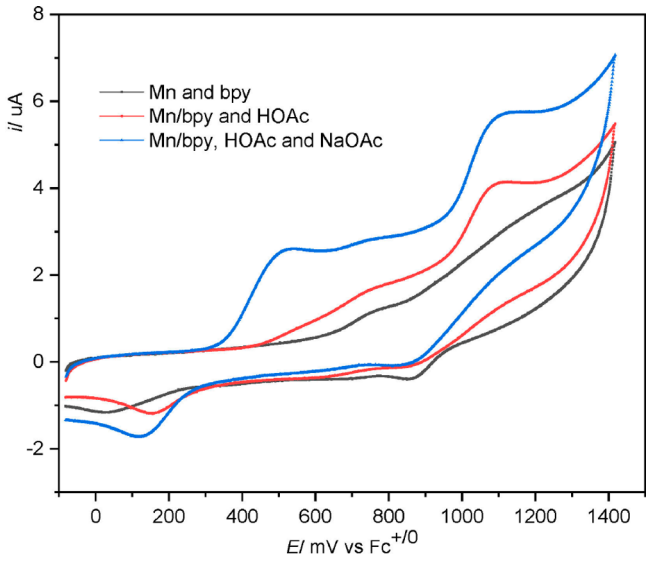

Figure 1. Cyclic voltammograms of Mn showing the effect of bpy and acetate on the catalyst oxidation. Conditions: glassy carbon as working electrode, $Ag/AgNO_3$ reference electrode, and a platinum wire counter electrode. $LiClO_4$ (0.10 M in MeCN), $Mn(OTf)_2$ (1.0 mM), bpy (1.2 mM), NaOAc (2.0 mM), HOAc (60 mM). Scan rate: 20 mV/s.

line). We assigned this peak to the Mn^{II}/Mn^{III} oxidation, which was facilitated by the redox active ligand.[17] The oxidation wave at ca. 1.1 V likely represents the further oxidation of Mn^{III} to Mn^{IV} or other higher valent species. This oxidation event is, however, irrelevant to catalysis and will not be discussed herein.

The addition of HOAc to the reaction system led to an additional oxidative wave at ca. 500 mV (red line). This wave further increases in intensity in the presence of NaOAc (blue line), which provides a larger concentration of OAc^-. To further identify these irreversible redox features, we carried out differential pulse voltammetry experiments (DPV; Figure 2). The appearance of the oxidative wave at 500 mV in the presence of acetate is clearly observed (red and blue lines). These data revealed that OAc^- likely served as an additional ligand on Mn and reduced the potential needed for its oxidation. Previous electrolysis experiments under a constant anodic potential (Table 1, entry 6) revealed that the catalytic reaction requires a potential input of no more than 620 mV. Therefore, we reasoned that the oxidative feature at 500 mV is the key catalytic species that is responsible for the observed chloroalkylation reactivity.

Intriguingly, the addition of an additional equivalent of bpy (Mn/bpy = 1:2.4) to the catalytic mixture led to decreased intensity of the peak at 500 mV, while the peak at 700 mV became more pronounced (Figure 2, green line). It is likely that excessive bpy led to the formation of $Mn(bpy)_n$ ($n > 1$), which is more difficult to oxidize and less relevant to catalysis.

DOI: 10.1021/acscatal.8b03209
ACS Catal. 2019, 9, 746−754

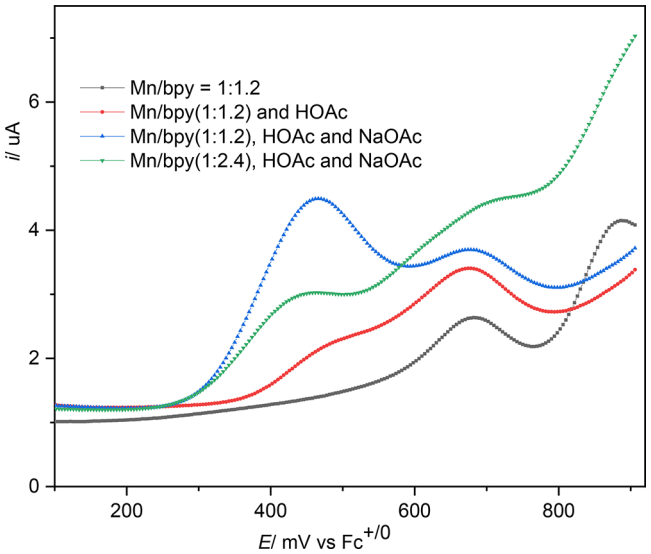

Figure 2. Differential pulse voltammograms of Mn showing the effect of bpy and acetate on the catalyst oxidation. Conditions: glassy carbon as working electrode, $Ag/AgNO_3$ reference electrode, and a platinum wire counter electrode. $LiClO_4$ (0.10 M in MeCN), $Mn(OTf)_2$ (3.0 mM), bpy (3.6 or 7.2 mM), NaOAc (4.0 mM), HOAc (60 mM). Scan rate: 20 mV/s, step *E*: 4 (mV), pulse amplitude: 50 mV, pulse width: 50 ms, pulse period: 200 ms.

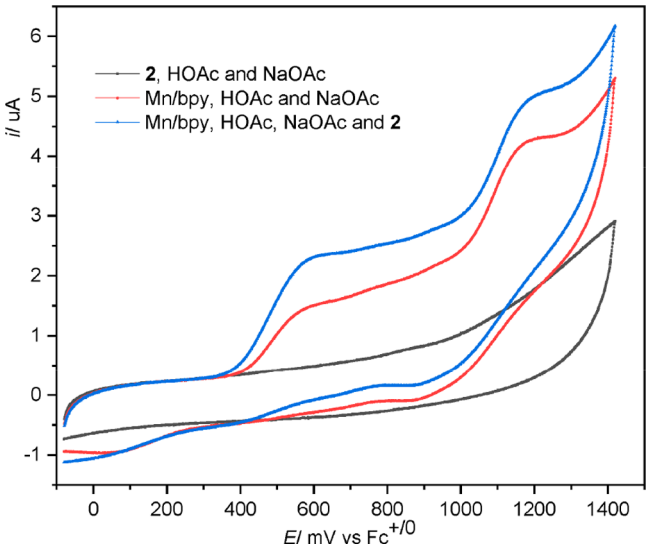

Figure 3. Cyclic voltammograms of the reaction system showing the catalytic effect of Mn in the oxidation of **2**. Conditions: glassy carbon as working electrode, $Ag/AgNO_3$ reference electrode, and a platinum wire counter electrode. $LiClO_4$ (0.10 M in MeCN), $Mn(OTf)_2$ (1.0 mM), bpy (1.2 mM), NaOAc (2.0 mM), **2** (5.0 mM), HOAc (60 mM). Scan rate: 20 mV/s.

Taken together, we hypothesize that the active Mn catalyst in our reaction adopts a formula of $[Mn^{III}(bpy)(OAc)_n(MeCN)_m]$ (n, m > 0, the net charge of the complex depends on n). Structurally analogous Mn(bpy) complexes have been used in reductive electrocatalysis (e.g., CO_2 reduction[18]) in their low oxidation states (formally $Mn^{I/-I}$). Literature data for the characterization of Mn^{III} complexes are largely limited to the solid-state structures.[6b,19] The preliminary electrochemical characterization of the catalyst in action in the chloroalkylation will thus serve as the foundation for our ongoing mechanistic investigation of related electrochemical transformations catalyzed by Mn.[10]

We then studied the role Mn plays in the formation of carbon-centered radical **IV**. Malononitrile **2** alone does not show any anodic feature in the potential window of 0−1.0 V (Figure 3, black line), showing that its direct oxidation on the anode is difficult and unlikely to happen under reaction conditions with an anodic potential of less than 650 mV. The addition of **2** to the $Mn/bpy/OAc^-$ mixture resulted in moderate current enhancement of the anodic peak at 500 mV (blue vs red lines). Increasing the concentration of **2**, however, did not result in further improvement of the catalytic current. We reasoned that the Mn^{III} catalyst generated electrochemically can form an adduct with **2** through coordination to a CN group or the α-carbon. The decomposition of this adduct to generate free radical **IV** is slow on the CV time scale and a catalytic current is thus not observed. In addition to being a ligand to Mn, we speculated that the acetate ion also accelerated the oxidation of **2** by functioning as a general base. In the standard electrolysis in an undivided cell, exogenous NaOAc was unnecessary because acetate was generated in situ on the Pt cathode during the reduction of HOAc to H_2.

The addition of Cl^- to the catalytic mixture also led to current increase at ca. 500 mV (Figure 4, blue vs red lines). We assign the new anodic wave to the oxidation of $[Mn^{II}]-Cl$ to

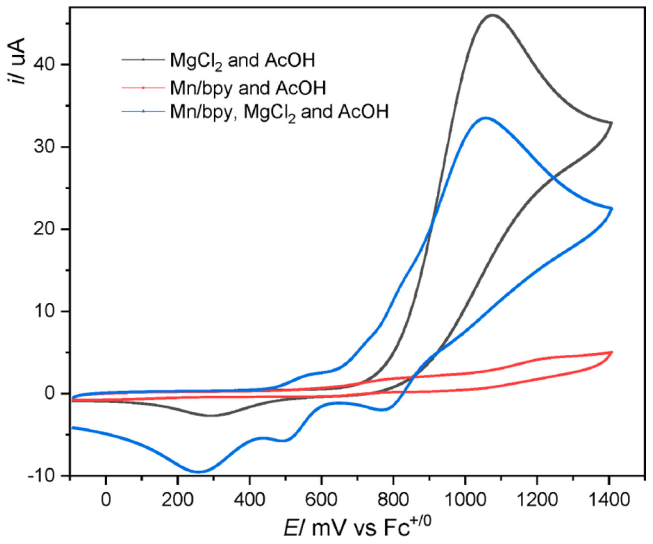

Figure 4. Cyclic voltammograms showing the effect of Mn in the oxidation of Cl^-. Conditions: glassy carbon as working electrode, $Ag/AgNO_3$ reference electrode, and a platinum wire counter electrode. $LiClO_4$ (0.10 M in MeCN), $Mn(OTf)_2$ (1.0 mM), bpy (1.2 mM), $MgCl_2$ (5.0 mM), HOAc (60 mM). Scan rate: 20 mV/s.

$[Mn^{III}]-Cl$.[10c] This redox event is quasi-reversible; the reduction of the catalytic active $[Mn^{III}]-Cl$ partially contributes to the cathodic wave at 500 mV. $MgCl_2$ alone does not display any oxidation wave at a potential smaller than 700 mV (black line), indicating that its direct oxidation contributes minimally to the observed reactivity. In this study, more soluble $MgCl_2$ was used instead of NaCl. The latter salt shows the same CV pattern, but the catalytic current is substantially less pronounced.

The very similar oxidation potential needed for the generation of **IV** and $[Mn^{III}]-Cl$ is unlikely a coincidence. Given that both anodic events are mediated by the Mn/bpy/

DOI: 10.1021/acscatal.8b03209
ACS Catal. 2019, 9, 746−754

OAc^- catalytic system, the potentials at which **IV** and $[Mn^{III}]$–Cl are generated are largely dependent upon the catalyst oxidation. These findings are consistent with the controlled potential electrolysis experiment wherein the application of 620 mV anodic potential proved sufficient in promoting the desired chloroalkylation reaction (see Table 1, entry 6).[20]

Taken together, all experimental data are in agreement with the mechanistic scenario detailed in Scheme 7. Anodically coupled electrolysis enabled the generation of carbon-centered radical **IV** and latent chlorine radical $[Mn^{III}–Cl]$ spontaneously. Both processes were mediated by the Mn catalyst. The alkene substrate first reacted with transient free radical **IV** to form **V**. This nascent transient radical subsequently cross coupled with $[Mn^{III}–Cl]$, a persistent open-shell intermediate, in a manner akin to metal-mediated atom transfer to provide the heterodifunctionalized product. Acetate generated on the cathode via the reduction of HOAc diffused to the bulk solution and facilitated the generation of **IV** as both a ligand to Mn and a proton acceptor.

Scheme 7. Proposed Mechanism Involving Catalytic, Anodically Coupled Electrolysis

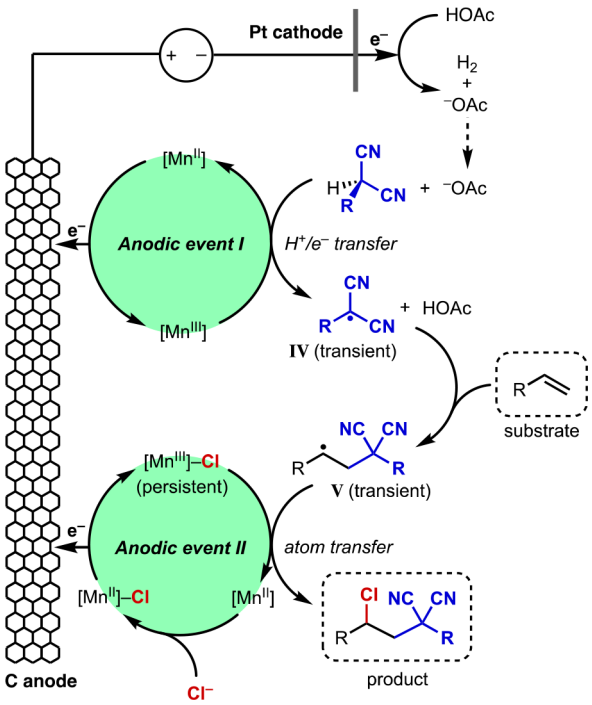

CONCLUSIONS

In conclusion, we report the oxidative chloroalkylation of alkenes via anodically coupled electrolysis. Malononitrile derivatives and NaCl were used as the reagents and activated via parallel, Mn-catalyzed electrochemical oxidation processes. The resulting open-shell intermediates react with the alkene in a selective fashion, yielding the heterodifunctionalization products in high efficiency across a broad scope of substrates. Current efforts are focused on the mechanistic investigation of anodically coupled electrolysis and the further application of this new synthetic strategy in reaction discovery and organic synthesis.

ASSOCIATED CONTENT

Supporting Information

The Supporting Information is available free of charge on the ACS Publications website at DOI: 10.1021/acscatal.8b03209.

Experimental procedures and characterization data (PDF)

Crystallographic data for **19** (CIF)

AUTHOR INFORMATION

Corresponding Author

*E-mail: songlin@cornell.edu.

ORCID

Song Lin: 0000-0002-8880-6476

Notes

The authors declare no competing financial interest.

ACKNOWLEDGMENTS

Financial support was provided by Cornell University, NSF (CHE-1751839; for reaction development), and NIGMS (R01GM130928; for mechanistic study). This study made use of the Cornell Center for Materials Research (CCMR) Shared Facilities (DMR-1719875) and the NMR facility (CHE-1531632) supported by NSF. We thank CCMR for supporting A.R.A.'s REU (DMR-1460428 and DMR-1719875) and Prof. Kazuhiro Chiba for supporting A.O.'s research internship at Cornell University. We are grateful to Dr. Samantha MacMillan for help with X-ray crystal structure collection and determination.

REFERENCES

(1) For representative reviews, see: (a) Chemler, S. R.; Fuller, P. H. Heterocycle Synthesis by Copper Facilitated Addition of Heteroatoms to Alkenes, Alkynes and Arenes. *Chem. Soc. Rev.* **2007**, *36*, 1153–1160. (b) McDonald, R. I.; Liu, G.; Stahl, S. S. Palladium(II)-Catalyzed Alkene Functionalization via Nucleopalladation: Stereochemical Pathways and Enantioselective Catalytic Applications. *Chem. Rev.* **2011**, *111*, 2981–3019. (c) Yin, G.; Mu, X.; Liu, G. Palladium(II)-Catalyzed Oxidative Difunctionalization of Alkenes: Bond Forming at a High-Valent Palladium Center. *Acc. Chem. Res.* **2016**, *49*, 2413–2423. (d) Courant, T.; Masson, G. Recent Progress in Visible-Light Photoredox-Catalyzed Intermolecular 1,2-Difunctionalization of Double Bonds via an ATRA-Type Mechanism. *J. Org. Chem.* **2016**, *81*, 6945–6952. (e) Romero, R. M.; Wöste, T. H.; Muñiz, K. Vicinal Difunctionalization of Alkenes with Iodine(III) Reagents and Catalysts. *Chem. - Asian J.* **2014**, *9*, 972–983. (f) Williamson, K. S.; Michaelis, D. J.; Yoon, T. P. Advances in the Chemistry of Oxaziridines. *Chem. Rev.* **2014**, *114*, 8016–8036. (g) Derosa, J.; Tran, V. T.; van der Puyl, V. A.; Engle, K. M. Carbon–Carbon π-Bonds as Conjunctive Reagents in Cross-Coupling. *Aldrichimica Acta* **2018**, *51*, 21–32. (h) Lan, X.-W.; Wang, N.-X.; Xing, Y. Recent Advances in Radical Difunctionalization of Simple Alkenes. *Eur. J. Org. Chem.* **2017**, *2017*, 5821–5851.

(2) For examples of intermolecular haloalkylation of alkenes, see: (a) Wallentin, C.-J.; Nguyen, J. D.; Finkbeiner, P.; Stephenson, C. R. J. Visible Light-Mediated Atom Transfer Radical Addition via Oxidative and Reductive Quenching of Photocatalysts. *J. Am. Chem. Soc.* **2012**, *134*, 8875–8884. (b) Chen, B.; Fang, C.; Liu, P.; Ready, J. M. Rhodium-Catalyzed Enantioselective Radical Addition of CX4 Reagents to Olefins. *Angew. Chem., Int. Ed.* **2017**, *56*, 8780–8784. (c) Yang, D.; Gu, S.; Yan, Y.-L.; Zhu, N.-Y.; Cheung, K.-K. Highly Enantioselective Atom-Transfer Radical Cyclization Reactions Catalyzed by Chiral Lewis Acids. *J. Am. Chem. Soc.* **2001**, *123*, 8612–8613. (d) Curran, D. P.; Chen, M. H.; Spletzer, E.; Seong, C. M.; Chang, C. T. Atom Transfer Addition and Annulation Reactions of Iodomalo-

DOI: 10.1021/acscatal.8b03209
ACS Catal. 2019, 9, 746–754

nates. *J. Am. Chem. Soc.* **1989**, *111*, 8872−8878. (e) Beniazza, R.; Douarre, M.; Lastécouères, D.; Vincent, J.-M. Metal-Free and Light-Promoted Radical Iodotrifluoromethylation of Alkenes with Togni Reagent as the Source of CF_3 and Iodine. *Chem. Commun.* **2017**, *53*, 3547−3550. (f) Dengiz, C.; Caliskan, R.; Balci, M. Chloroacetonylation of C = C Double Bonds Promoted by Manganese(III) Acetate. *Tetrahedron Lett.* **2012**, *53*, 550−552. (g) Nguyen, J. D.; Tucker, J. W.; Konieczynska, M. D.; Stephenson, C. R. J. Intermolecular Atom Transfer Radical Addition to Olefins Mediated by Oxidative Quenching of Photoredox Catalysts. *J. Am. Chem. Soc.* **2011**, *133*, 4160−4163.

(3) Early examples of Kharasch addition using radical initiators: (a) Kharasch, M. S.; Jensen, E. V.; Urry, W. H. Addition of Carbon Tetrachloride and Chloroform to Olefins. *Science* **1945**, *102*, 128. (b) Kharasch, M. S.; Skell, P. S.; Fisher, P. Reactions of Atoms and Free Radicals in Solution. XII. The Addition of Bromo Esters to Olefins. *J. Am. Chem. Soc.* **1948**, *70*, 1055−1059.

(4) Representative reviews on metal-catalyzed atom-transfer radical additions: (a) Iqbal, J.; Bhatia, B.; Nayyar, N. K. Transition Metal-Promoted Free-Radical Reactions in Organic Synthesis: The Formation of Carbon-Carbon Bonds. *Chem. Rev.* **1994**, *94*, 519−564. (b) Clark, A. J. Atom Transfer Radical Cyclisation Reactions Mediated by Copper Complexes. *Chem. Soc. Rev.* **2002**, *31*, 1−11. (c) Pintauer, T.; Matyjaszewski, K. Atom Transfer Radical Addition and Polymerization Reactions Catalyzed by ppm Amounts of Copper Complexes. *Chem. Soc. Rev.* **2008**, *37*, 1087−1097. (d) Minisci, F. Free-Radical Additions to Olefins in the Presence of Redox Systems. *Acc. Chem. Res.* **1975**, *8*, 165−171. (e) Gossage, R. A.; van de Kuil, L. A.; van Koten, G. Diaminoarylnickel(II) "Pincer" Complexes: Mechanistic Considerations in the Kharasch Addition Reaction, Controlled Polymerization, and Dendrimeric Transition Metal Catalysts. *Acc. Chem. Res.* **1998**, *31*, 423−431. (f) Studer, A.; Curran, D. P. Catalysis of Radical Reactions: A Radical Chemistry Perspective. *Angew. Chem., Int. Ed.* **2016**, *55*, 58−102.

(5) For examples, see: (a) Yang, D.; Yan, Y.-L.; Zheng, B.-F.; Gao, Q.; Zhu, N.-Y. Copper(I)-Catalyzed Chlorine Atom Transfer Radical Cyclization Reactions of Unsaturated α-Chloro β-Keto Esters. *Org. Lett.* **2006**, *8*, 5757−5760. (b) Snider, B. B.; Patricia, J. J.; Kates, S. A. Mechanism of Manganese(III)-Based Oxidation of β-Keto Esters. *J. Org. Chem.* **1988**, *53*, 2137−2143. (c) Hayes, T. K.; Villani, R.; Weinreb, S. M. Exploratory Studies of the Transition Metal Catalyzed Intramolecular Cyclization of Unsaturated α,α-Dichloro Esters, Acids, and Nitriles. *J. Am. Chem. Soc.* **1988**, *110*, 5533−5543. (d) Ng, F.-N.; Lau, Y.-F.; Zhou, Z.; Yu, W.-Y. [Rh^{III}(Cp*)]-Catalyzed Cascade Arylation and Chlorination of α-Diazocarbonyl Compounds with Arylboronic Acids and N-Chlorosuccinimide for Facile Synthesis of α-Aryl-α-chloro Carbonyl Compounds. *Org. Lett.* **2015**, *17*, 1676−1679. (e) Bellus, D. Copper-Catalyzed Additions of Organic Polyhalides to Olefins: A Versatile Synthetic Tool. *Pure Appl. Chem.* **1985**, *57*, 1827−1838. (f) McGonagle, F. I.; Brown, L.; Cooke, A.; Sutherland, A. A Three-Step Tandem Process for the Synthesis of Bicyclic γ-Lactams. *Org. Biomol. Chem.* **2010**, *8*, 3418−3425. An example using less reactive, monochlorinated substrate under high temperature: (g) Lee, G. M.; Parvez, M.; Weinreb, S. M. Intramolecular Metal Catalyzed Kharasch Cyclizations of Olefinic α-Halo Esters and Acids. *Tetrahedron* **1988**, *44*, 4671−4678.

(6) For representative reviews, see: (a) Snider, B. B. Manganese (III)-Based Oxidative Free-Radical Cyclizations. *Chem. Rev.* **1996**, *96*, 339−363. (b) Snider, B. B. Mechanisms of $Mn(OAc)_3$-Based Oxidative Free-Radical Additions and Cyclizations. *Tetrahedron* **2009**, *65*, 10738−10744.

(7) For examples, see: (a) Corey, E. J.; Kang, M. New and General Synthesis of Polycyclic γ-Lactones by Double Annulation. *J. Am. Chem. Soc.* **1984**, *106*, 5384−5385. (b) Snider, B. B.; Mohan, R.; Kates, S. A. Manganese(III)-Based Oxidative Free-Radical Cyclization. Synthesis of (±)-Podocarpic Acid. *J. Org. Chem.* **1985**, *50*, 3659−3661. (c) Ernst, A. B.; Fristad, W. E. Intramolecular Lactone Annulation of Activated Acids with Mn(III). *Tetrahedron Lett.* **1985**, *26*, 3761−3764. (d) Kates, S. A.; Dombroski, M. A.; Snider, B. B. Manganese(III)-Based Oxidative Free-Radical Cyclization of Unsaturated β-Keto Esters, 1,3-Diketones, and Malonate Diesters. *J. Org. Chem.* **1990**, *55*, 2427−2436. (e) Phillips, E. M.; Roberts, J. M.; Scheidt, K. A. Catalytic Enantioselective Total Syntheses of Bakkenolides I, J, and S: Application of a Carbene-Catalyzed Desymmetrization. *Org. Lett.* **2010**, *12*, 2830−2833. (f) Wang, X.; Ma, Z.; Lu, J.; Tan, X.; Chen, C. Asymmetric Synthesis of Ageliferin. *J. Am. Chem. Soc.* **2011**, *133*, 15350−15353.

(8) Related to our work, Mn-mediated radical cyclization with 1,3-dicarbonyls has also been achieved under electrochemical conditions. See:(a) Snider, B. B.; McCarthy, B. A. Mn(III)-Mediated Electrochemical Oxidative Free-Radical Cyclizations. In *Benign by Design*; ACS Symposium Series; American Chemical Society, 1994; Vol. *577*, pp 7−84. (b) Merchant, R. R.; Oberg, K. M.; Lin, Y.; Novak, A. J. E.; Felding, J.; Baran, P. S. Divergent Synthesis of Pyrone Diterpenes via Radical Cross Coupling. *J. Am. Chem. Soc.* **2018**, *140*, 7462−7465. (c) Shundo, R.; Nishiguchi, I.; Matsubara, Y.; Hirashima, T. Mn^{3+}-Mediated Coupling-Cyclization of 5-Arylpent-1-enes with Active Methylene Compounds by Electrooxidation. *Chem. Lett.* **1991**, *20*, 235−236. (d) Shundo, R.; Nishiguchi, I.; Matsubara, Y.; Hirashima, T. Carbon—Carbon Bond Formation Using Manganese(III) Acetate as an Electrochemical Mediator. *Tetrahedron* **1991**, *47*, 831−840.

(9) For representative recent reviews on electrosynthesis, see: (a) Moeller, K. D. Synthetic Applications of Anodic Electrochemistry. *Tetrahedron* **2000**, *56*, 9527−9554. (b) Sperry, J. B.; Wright, D. L. The Application of Cathodic Reductions and Anodic Oxidations in the Synthe-sis of Complex Molecules. *Chem. Soc. Rev.* **2006**, *35*, 605−621. (c) Yoshida, J.; Kataoka, K.; Horcajada, R.; Nagaki, A. Modern Strategies in Electroorganic Synthesis. *Chem. Rev.* **2008**, *108*, 2265−2299. (d) Francke, R.; Little, R. D. Redox Catalysis in Organic Electrosynthesis: Basic Principles and Recent Developments. *Chem. Soc. Rev.* **2014**, *43*, 2492−2521. (e) Yan, M.; Kawamata, Y.; Baran, P. S. Synthetic Organic Electrochemical Methods Since 2000: On the Verge of a Renaissance. *Chem. Rev.* **2017**, *117*, 13230−13319. (f) Möhle, S.; Zirbes, M.; Rodrigo, E.; Gieshoff, T.; Wiebe, A.; Waldvogel, S. R. Modern Electrochemical Aspects for the Synthesis of Value-Added Organic Products. *Angew. Chem., Int. Ed.* **2018**, *57*, 6018−6041. (g) Mitsudo, K.; Kurimoto, Y.; Yoshioka, K.; Suga, S. Miniaturization and Combinatorial Approach in Organic Electrochemistry. *Chem. Rev.* **2018**, *118*, 5985−5999. (h) Tang, S.; Liu, Y.; Lei, A. Electrochemical Oxidative Cross-Coupling with Hydrogen Evolution: A Green and Sustainable Way for Bond Formation. *Chem.* **2018**, *4*, 27−45. (i) Sauermann, N.; Meyer, T. H.; Qiu, Y.; Ackermann, L. Electrocatalytic C−H Activation. *ACS Catal.* **2018**, *8*, 7086−7103. (j) Sauermann, N.; Meyer, T. H.; Ackermann, L. Electrochemical Cobalt-Catalyzed C−H Activation. *Chem. - Eur. J.* **2018**, *24*, 16209.

(10) Perspectives: (a) Sauer, G. S.; Lin, S. An Electrocatalytic Approach to the Radical Difunctionalization of Alkenes. *ACS Catal.* **2018**, *8*, 5175−5187. (b) Parry, J. B.; Fu, N.; Lin, S. Electrocatalytic Difunctionalization of Olefins as a General Approach to the Synthesis of Vicinal Diamines. *Synlett* **2018**, *29*, 257−265. Examples: (c) Ye, K.; Pombar, G.; Fu, N.; Sauer, G. S.; Keresztes, I.; Lin, S. Anodically Coupled Electrolysis for the Heterodifunctionalization of Alkenes. *J. Am. Chem. Soc.* **2018**, *140*, 2438−2441. (d) Fu, N.; Sauer, G. S.; Lin, S. Electrocatalytic Radical Dichlorination of Alkenes with Nucleophilic Chlorine Sources. *J. Am. Chem. Soc.* **2017**, *139*, 15548−15553. (e) Fu, N.; Sauer, G. S.; Saha, A.; Loo, A.; Lin, S. Metal-Catalyzed Electrochemical Diazidation of Alkenes. *Science* **2017**, *357*, 575−579.

(11) Reviews on persistent radical effect: (a) Studer, A. The Persistent Radical Effect in Organic Synthesis. *Chem. - Eur. J.* **2001**, *7*, 1159−1164. (b) Fischer, H. The Persistent Radical Effect: A Principle for Selective Radical Reactions and Living Radical Polymerizations. *Chem. Rev.* **2001**, *101*, 3581−3610. (c) Yan, M.; Lo, J. C.; Edwards, J. T.; Baran, P. S. Radicals: Reactive Intermediates with Translational Potential. *J. Am. Chem. Soc.* **2016**, *138*, 12692−12714.

(12) Our preliminary mechanistic studies revealed that in our Mn-catalyzed alkene difunctionalizations, the homolysis of the C═C π-bond induced by radical addition is usually the rate-limiting step. The

DOI: 10.1021/acscatal.8b03209
ACS Catal. 2019, 9, 746−754

radical group transfer to the resultant carbon-centered radical is usually facile.
(13) Smith, J. A.; Moeller, K. D. Oxidative Cyclizations, the Synthesis of Aryl-Substituted C-Glycosides, and the Role of the Second Electron Transfer Step. *Org. Lett.* **2013**, *15*, 5818−5821.
(14) Tsai, T.-Y.; Shia, K.-S.; Liu, H.-J. A Facile Method for the Construction of Highly Substituted Acetonitriles and Olefins. Malononitriles as Acetonitrile Carbanion and Alkylidene Dianion Equivalents. *Synlett* **2003**, 97−101.
(15) Mayr, H.; Kempf, B.; Ofial, A. R. π-Nucleophilicity in Carbon−Carbon Bond-Forming Reactions. *Acc. Chem. Res.* **2003**, *36*, 66−77.
(16) For the CV of $Mn(OTf)_2$, see ref 10d. For the CV of **2**, see Figure 2.
(17) Morrison, M. M.; Sawyer, D. T. Redox Chemistry of the Polyimine Complexes of Manganese (II), -(III), and-(IV) in Acetonitrile. *Inorg. Chem.* **1978**, *17*, 333−337.
(18) Sampson, M. D.; Kubiak, C. P. Manganese Electrocatalysts with Bulky Bipyridine Ligands: Utilizing Lewis Acids To Promote Carbon Dioxide Reduction at Low Overpotentials. *J. Am. Chem. Soc.* **2016**, *138*, 1386−1393.
(19) Fristad, W. E.; Peterson, J. R. Manganese(III)-Mediated γ-Lactone Annulation. *J. Org. Chem.* **1985**, *50*, 10−18.
(20) The reaction could take place at an applied anodic potential as low as 500 mV vs $Fc^{+/0}$ at the expense of a lower rate.

DOI: 10.1021/acscatal.8b03209
ACS Catal. 2019, 9, 746−754